Evaluation of Machine Learning Models for Mapping Food Crops using Sentinel-2A Imagery in West Java, Indonesia

Riki Ridwana[1,2], Muhammad Kamal[3], Sanjiwana Arjasakusuma[3], and Muh Fiqri Abdi Rabbi[4]

[1]Mapping Survey and Geographic Information Study Program, Faculty of Social Sciences Education, Universitas Pendidikan Indonesia, Jl. Dr. Setiabudhi No. 229, Bandung, Indonesia
[2]Doctoral Program in Geography, Faculty of Geography, Universitas Gadjah Mada, Yogyakarta, Indonesia
[3]Departement of Geography Information Science, Faculty of Geography, Universitas Gadjah Mada, Bulaksumur, Yogyakarta 55281, Indonesia
[4]Geography Information Science Study Program, Faculty of Social Sciences Education, Universitas Pendidikan Indonesia, Jawa Barat, Indonesia.

Abstract. Data on the distribution patterns and locations of food crops are crucial for monitoring and controlling the sustainability of agricultural resources and guaranteeing food security. Plant classification based on machine learning has been widely used to detect food crop areas. However, there are still challenges in mapping plant types and plant area effectively and efficiently. The aim of this research is to evaluate machine learning models in mapping and calculating the area of food crops (**rice**) in West Java Province, Indonesia. Google Earth Engine is used in this study as a big data cloud computing platform for remote sensing. Normalized Difference Vegetation Index (NDVI) and Enhanced Vegetation Index (EVI) Sentinel-2A imagery is utilized to employ time series data as input characteristics for the three most popular machine learning models: Support Vector Machine (SVM), Random Forest (RF), and Classification and Regression Trees (CART). The research results show that the three machine learning models are able to map and calculate the area of food crops in West Java, Indonesia. The RF algorithm produces the highest overall accuracy rate (98.51%) and is the fastest in the accuracy assessment and image classification process compared to the SVM and CART algorithms.

1 Introduction

The quick expansion of world urbanization and population is pressing for food production from limited agricultural resources to maintain food security [1-4]. In order to satisfy the demands for food supply, a large number of sophisticated agricultural systems have been developed with careful monitoring and management of agricultural resources to boost efficiency and crop yields [5-7]. Monitoring and managing sustainable agricultural resources greatly benefits from knowing the locations and patterns of food crop distribution [8-11]. This information is used as a basis for policy makers in estimating harvest yields [12,13], Estimated crop specific water consumption [14-16], disaster assessment [17, 18], and ensuring balanced regional food security [19, 20]. Consequently, crop maps are a trustworthy tool for sustainable agriculture management that decision makers may rely on.

So far, spatial information on plant types and planting areas still uses traditional methods, namely based on field surveys, area unit frameworks, and statistical reports, which take a lot of time, are labor intensive, cost a lot of money, and lack timely data updates [21–23]. On the other hand, Nowadays, plant kinds may be reliably mapped using remote sensing technology, which offers broad coverage capabilities, quick data collecting, and cost and human resource savings [24-26]. Although methods for mapping plant types in the last two decades have been developed using different remote sensing data [27–29], There are still gaps and challenges to develop remote sensing technology.

One of these challenges is the limitation between image data quality and linearly correlated costs [30–33]. The simultaneous consideration of spatial, spectral, and temporal image resolution is necessary when employing remote sensing data for mapping plant species [30-34], because the main priority is to use high quality data but at low cost. For example, Himawari-8 data has been widely used in the last decade, even though it is free to access, the spatial resolution is too coarse [35], similar to MODIS data only suitable for land area of more than 32 ha [36], so its application in mapping plant types is very limited. Landsat imagery overcomes this challenge, however the spatial resolution is still unable to capture the true spatial distribution on fragmented agricultural land, for example for land areas of less than 0.5 ha. In addition, Landsat's temporal resolution of 16 days is insufficient to capture information about the phenology of different plants [37].

High or very hight resolution commercial imagery and hyperspectral sensors offer a wealth of information about plant texture and structure and are capable of mapping plant types across complex landscapes and growing area conditions [38, 39]. However, its use is limited by large costs and requires enormous amounts of data storage and complex computing needs [40]. Another option uses RADAR data with its ability to penetrate clouds and is not affected by weather conditions [41-43], However, it has a high noise level and is also expensive [44]. So from this side of the problem, Sentinel-2 imagery can be used as an alternative solution with a spatial capability of 10 meters, a temporal resolution of 5 days and a spectral resolution that is considered good for plant mapping [45-47].

The next challenge in mapping plant types using remote sensing technology is agronomic factors. Each plant has a unique growth phase. It will be more advantageous to begin the crop-planting portion of the growing season as early as possible in order to control production, track crop yields, and forecast trends in food prices [48, 49]. Considering that different plant growth phases overlap with each other, During the overlap period, the spectral response of many plant species may be identical. At that time, with complex climatic and environmental conditions, the growth conditions for the same type of plant could vary, resulting in the number of classes increasing, which could reduce mapping accuracy.

Looking at the factors above, research generally focuses on mapping plant types by utilizing data from all growth phases or critical growth periods. Research that uses data from all phases of plant growth for mapping includes [50-52], most of them combine vegetation index curves as the most interesting features. Classification algorithms are another challenge because they can affect the level of accuracy of mapping plant types [53-57]. Over the last few decades, machine learning techniques such as Random Forest (RF), Support Vector Machine (SVM), Classification, and Regression Trees (CART) have been utilized, and others have been very good at classifying plant types, despite the fact that they only perform hard classification on each pixel without taking the characteristics of neighboring pixels into consideration. because of its ability to classify large image sets using known data and spatial data assisted by field data [53, 58–61].

Based on the background above, This study's objective is to assess the ability of the SVM, RF, CART algorithm machine learning model in mapping rice plant types in tropical areas, namely West Java Province, Indonesia, using Sentinel-2A imagery. In an effort to increase mapping accuracy, the plant type classification stage is supported by vegetation index transformation, namely normalized difference vegetation index (NDVI) and enhanced vegetation index (EVI) as input features.

2 Method

2.1 Location

The study was carried out in West Java Province, which is situated in the western region of Indonesia's Java Island. Geographically, it is located at 108°1'-108°41'E and 5°50'-7°50'S, bordering DKI Jakarta and the Java Sea to the north, the Indian Ocean to the south, Banten Province and DKI Jakarta to the west, the Java Sea and Central Java Province to the east. The area of West Java Province is 35,378 km^2, the map of which can be seen in figure 1. This location was chosen because West Java is one of the national rice barns, almost 23% of the total area is allocated for paddy/rice production. West Java Province's agricultural products contribute 15% of Indonesia's total agricultural value. One of the most widely produced food crops in West Java is rice [62].

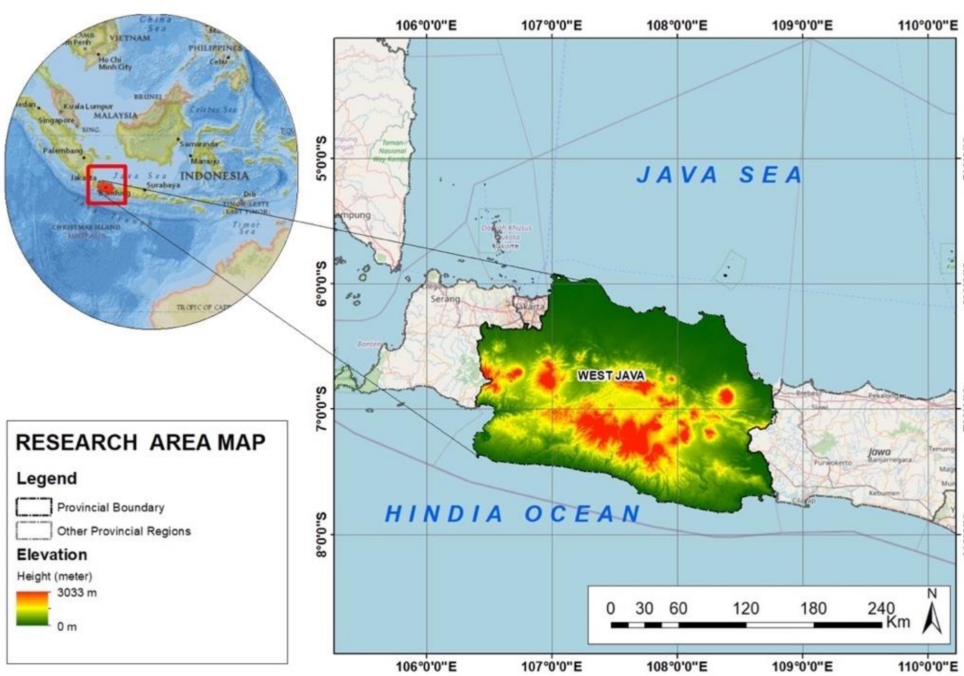

Fig. 1. Map of research location, West Java Province (Source: Data Processing, 2023)

2.2 Research Materials and Tools

The data used is Sentinel-2A with a spatial resolution of 10 m. All data is available from the beginning to the end of 2022 and is filtered by <20% cloud-free imagery obtained during the October to December rice planting season. Then the data is processed via Google Earth

Engine (https://earthengine.google.com/). L2A level lower atmosphere (BOA) reflectance data is used. Then the Sentinel-2 data were resampled to 10 m resolution with bilinear sampling. The red edge band and the initial 60 m resolution band are then eliminated. Ultimately, this piece used six bands: Band 2, Band 3, Band 4, Band 8, Band 11, and Band 12.

Other data used are the administrative boundaries in the shp format of West Java Province as the research locus which is then carried out a masking process on the Sentinel image scene. Obtained through the Indonesian homeland geoportal owned by the Geospatial Information Agency. Validation data for modeling food crops using image data with higher spatial resolution comes from Google Earth. Data collection tools used in this research include a laptop, Google Earth Engine web application, a set of stationery, etc.

2.3 Mapping Techniques

The first mapping technique carried out visual interpretation of food plants in West Java. Second, extraction was applied to Sentinel time series features with Normalized Difference Vegetation Index (NDVI) and Enhanced Vegetation Index (EVI) transformations for food crop sample points. Then reconstruct the machine learning model consisting of the Support Vector Machine (SVM), Random Forest (RF), and Classification and Regression Trees (CART) algorithms. The classifier is fed the NDVI and EVI time series features and models, and the best model is chosen by comparing how well the results perform. The parameters for the SVM and RF classifiers are described in Table 1.

Table 1. Parameter description of the SVM, RF and CART classifiers.

Classifier	Parameter	Description
SVM	C	C is the penalty coefficient used to control the loss function.
	Gamma	gamma denotes the kernel function coefficient.
RF	n_estimators	n_estimators shows the ability and complexity of RF to learn from data.
	min_samples_split	min_samples_split expresses the minimum number of samples needed to split internal nodes.
	min_sampel_leaf	min_samples_leaf indicates the minimum sample tree the leaf nodes.
	max_features	max_features mean the number of features to be considered when finding the optimal splitting point.
CART	minsplit	The minimum number of observations that must exist in node for splitting to occur
	minbucket	Minimum number of observations at any terminal node (which is also equivalent to 1/3 of minsplit)
	maxcompete	The number of competitor splits retained in the output
	maxsurrogate	The number of replacement splits maintained in the output
	usesurrogate	Controls how surrogates are used in the model

Source: [63]

2.4 Mapping Validation

This study employed two metrics² the kappa coefficient and total accuracy² to assess how well machine learning algorithms performed [64]. Weighted averages were utilized to assess all parameters (https://scikit-learn.org/). Given the unbalanced samples, it is incorrect to provide the same weight to each class; however, the weighted average method gives each class a varied weight based on its size. The weight of each class is based on how many samples are in that class. The percentage of total classes that are successfully predicted is known as overall accuracy; consistency testing is done using the kappa coefficient, which shows the error matrix's balance.

$$\text{Overall Accuracy} = \frac{TP+TN}{TP+FP+FN+TN} \quad (1)$$

$$\text{Kappa Coefficient} = \frac{P0-Pe}{1-Pe} \quad (2)$$

Positive and negative represent the existence or absence of plants, in addition to TP and FP signifying true and false positive predictions and TN and FN signifying true and false negative predictions, respectively. In Table 2, the confusion matrix is displayed. The recall rate displays the proportion of correctly identified samples in a class, whereas the precision rate provides the percentage of data that is correctly classified overall. The confusion matrix's diagonal elements are represented by the ratio of p0 to all matrix elements, and the square of the number and the total of the products between the expected and actual data volumes for each category are represented by pe and p0, respectively.

Table 2. Confusion matrix charted by the predicted and actual classification

		Predicted	
		Positive	**Negative**
Actual	Positive	True positives (TP)	False negatives (FN)
	Negative	False positives (FP)	True negatives (TN)

Source: [63]

2.5 Evaluation of Machine Learning Models

This effectiveness evaluation is applied to a food crop mapping model using machine learning. The methods and approaches used to evaluate machine learning models are cost effectiveness [65] modified. For cost efficiency, three factors were taken into consideration: the expenses related to each mapping approach, as well as an accuracy assessment based on total accuracy. Table 3 shows the time and cost estimates for each component and subcomponent as well as the mapping strategy.

Table 3. Components and subcomponents used to estimate the costs and time associated with each mapping approach.

Components	**Subcomponents**
(1) Data acquisition and preparation*	Plant identification and database* Multivariate analysis and plant classification*
(2) Image data acquisition and preparation	Image acquisition Image preprocessing
(3) Image classification	SVM algorithm RF algorithm CART algorithm

Source: [66]

*shows consistent components for modeling

The confusion matrix was calculated for the paddy maps for the part of the accuracy assessment. The classes in the classified photos are matched using the training regions that are offered for accuracy testing. For every method, picture dataset, and spatial scale map, the overall accuracy is computed and the outcomes are examined.

The acquisition and preparation of validation data, the acquisition and preparation of image data, picture classification, and accuracy assessment are the four key components that determine processing time. The measurement of cost-effectiveness presupposes the existence of necessary gear and software. Each component and subcomponent's expenses and time are recorded in advance of the time-effectiveness analysis. Figure 2 displays the study methodology flowchart.

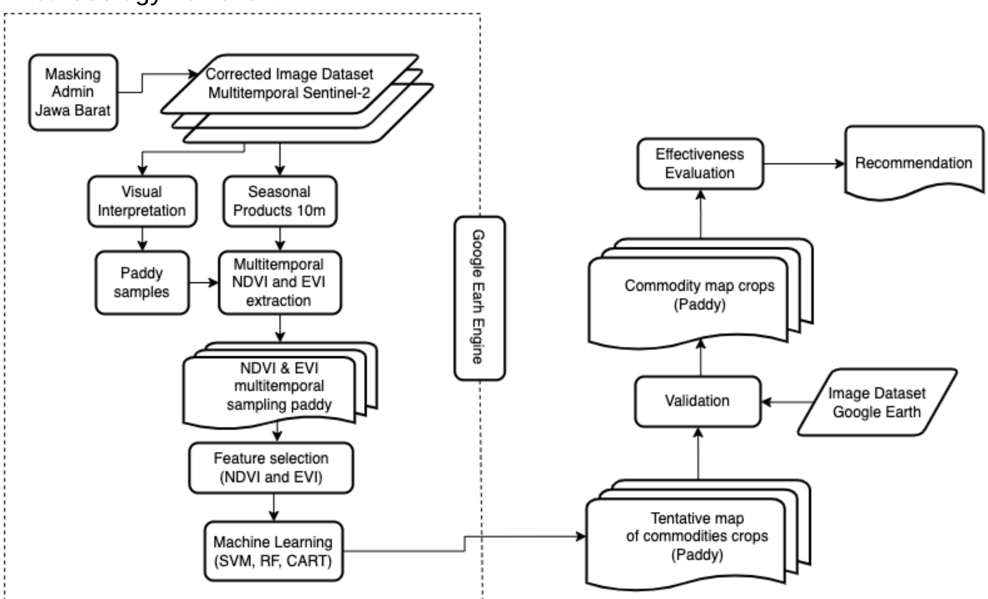

Fig. 2. Flowchart of the study methods

3 Result and Discussion

3.1 Feature Selection

Figure 3 is the Confusion Matrix result from the model, each of the SVM, Random Forest, and CART methods. For the model using the SVM method, it was found that the True Positive, False Positive, True Negative and False Negative numbers were 75, 17, 20, 78 and accordingly, as displayed in Table 2. The results above indicate that the error in classifying Food plant cover based on rice and non-rice categories is quite good although the True Positive number is still slightly smaller than the True Negative. Meanwhile, for other methods, namely Random Forest, the True Positive, False Positive, True Negative, and False Negative numbers are 43, 10, 20, and 48 respectively and the CART method is 47, 27, 42, and 17 respectively. When compared with all the models that have been developed in this study, it is known that the Random Forest method has a small error in classifying paddy based on the categories of meeting quality standards and not meeting quality standards where the number of false positives and false negatives is the smallest.

NDVI and EVI as input features are compared with each other to then choose which feature is the most optimal. Only one model classification result is shown since the two sets of features are fed into separate models to produce reasonably consistent results. Since the RF model has the highest accuracy variation and the lowest training time, its results are provided.

In this investigation, the two feature groups' categorization abilities differed significantly. Of all the characteristics, the optimized input feature (NDVI) has the highest accuracy (Table 4). The EVI function, however, has the least accuracy. When one of EVI's properties is compromised, the influence of clouds, fog, and insolation can lead to certain restrictions, but NDVI has additional features for plant classification, which increases the likelihood of accurate plant classification. To increase classification accuracy, NDVI will also provide the classifier access to more temporal features. In our later trials, we classified plants using NDVI data because it produced the best classification results.

Table **4**. Comparison of RF model results for paddy classification using two groups of features

	NDVI	**EVI**
Overall accuracy	0.4909	0.2364
Coefficient appa	0.4554	0.2223

3.2 Support Vector Machine, Random Forest, Classification and Regression Trees

The classification outcomes of machine learning classifiers are greatly influenced by their hyperparameter settings. In order to determine the hyperparameter, we employed a "random search" method. The best parameter chosen by the three classifiers is the RF hyperparameter. There are notable variations in the classification performance of these three classifiers (Figure 3).

RF outperformed the other two machine learning classifiers, achieving an accuracy of 98.51%. Higher classification accuracy is demonstrated by the RF model, which combines the properties of the original data with the output of another single model as input to make decisions. Nevertheless, accuracy will be decreased because the RF model is unable to determine whether the output of other models is accurate. Therefore, the confusion matrix of the stacking model shows non-optimal results for almost all classes. CART (97.01%) and SVM (85.58%) have slightly lower performance than RF and have a longer training time, because their high time complexity makes them unsuitable for large-scale data training.

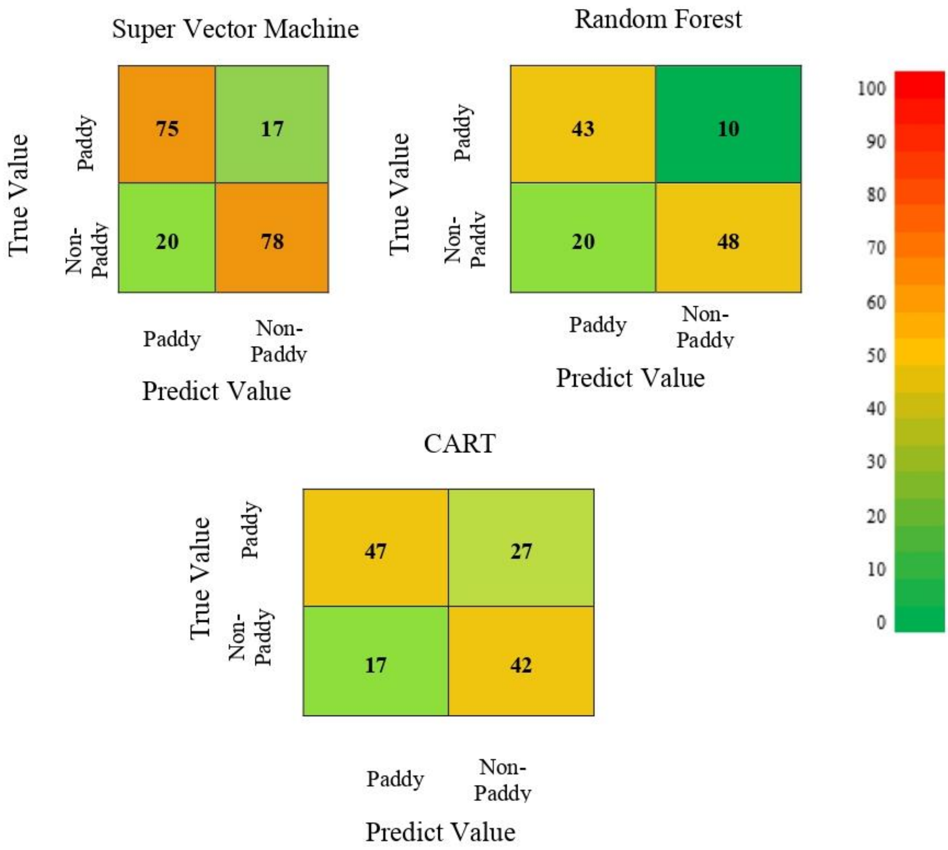

Fig. 3. Confusion matrix obtained by SVM (a), RF (b), and CART (c) models, using NDVI as input feature.

Both RF (98.51%) and CART (97.01%) attained comparable classification accuracy, and RF required less training time than CART. Compared to other models, it is evident that RF produces exceptional classification performance; SVM, on the other hand, performs the worst (Fig. 4). Choosing machine learning model hyperparameters can be challenging and time consuming, but due to the need to compare numerous hyperparameters, the accuracy of machine learning in this study is quite high.

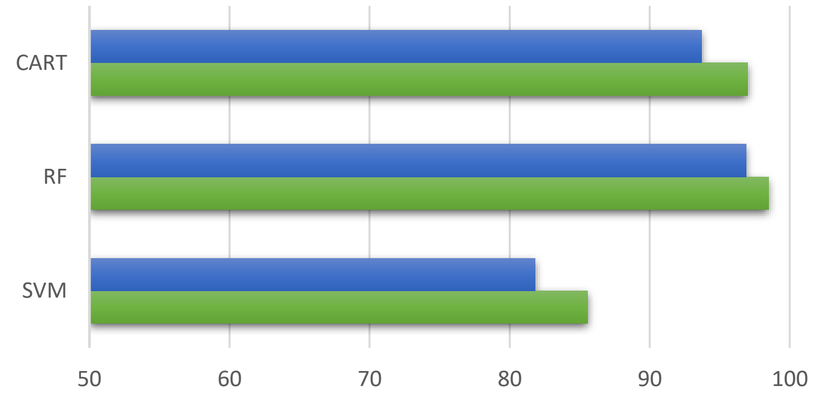

	SVM	RF	CART
Kappa Coefficient	81,83	96,88	93,71
Overall Accuracy	85,58	98,51	97,01

Fig. 4. Overall Accuracy and Kappa Coefficient (%) achieved by various classifiers using NDVI as input.

3.3 Effectiveness Evaluation Model Machine Learning

The RF approach produced the best classification results out of all the SVM, RF, and CART machine learning models (Fig. 4). In contrast, the SVM and CART learning methods have much lower performance than the RF learning method. The classification accuracy of SVM is the lowest among the three. A comparison is made between the SVM, RF and CART confusion matrices, each of which is the best performing machine learning model. In order to demonstrate the relative strengths of the two classifiers for each category, Table 5 shows the differences.

Tabel 5. Differences between the confusion matrices achieved by RF and CART classifiers

Reference Classes	Predict Classes	
	Paddy	Non-Paddy
Paddy	75	17
Non Paddy	20	68

Plots representing classification mistakes that lie outside the confusion matrix's diagonal can be categorized into many forms. These include: (1) Inaccuracies in dividing crops in rotation separated into groups that are non-rotational and rotational. (2) Inaccurate categorization of non-rotation crops. (3) Misclassification between different plants. The RF approach lowers the misclassification of non-rotation crops to rotation crops by 68 pixels and the misclassification of non-rotation crops amongst each other by 142 pixels when compared to SVM and CART. Table 5 shows that RF performs better than the RF and CART models in differentiating between rotation crops and non-rotation crops, with all values on the diagonal being positive and most values on the non-diagonal being negative. Thus, RF improves plant classification results significantly. The plots classified based on SVM, RF, and CART are shown in Figure 5.a

 https://doi.org/10.1051/e3sconf/202460003007

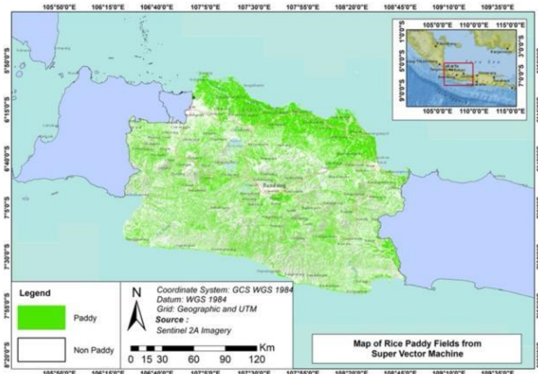

(a) SVM

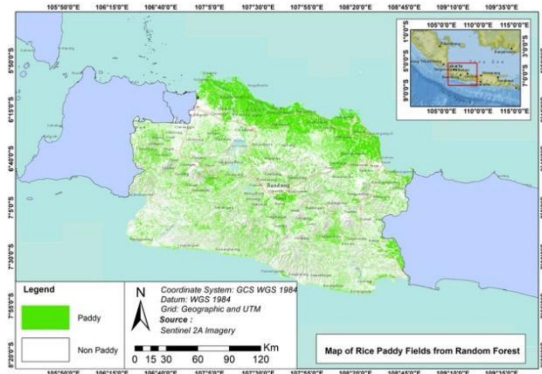

(b) RF

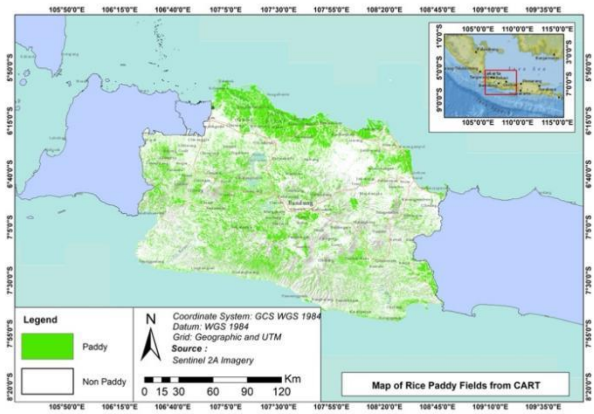

(c) CART

Fig. 5. Paddy Classification Map generated by SVM model (a), RF (b), CART (c).

Based on the four components of mapping model effectiveness (accuracy evaluation, image classification, validation data acquisition and preparation, and image data collection and preparation), Figure 6 presents the findings of the time effectiveness for the three study techniques. Overall, the three models used have the same processing time in terms of validation data acquisition and preparation, image data acquisition and preparation each is approximately only 10 seconds. The RF model was considered the most effective in rice mapping based on an experiment that only took 1 minute 2 seconds (accuracy assessment) and 18 seconds (image classification). These experiments were all implemented on the same device and internet connection speed, so it is likely that the results will be different if applied to different devices and internet connection speeds.

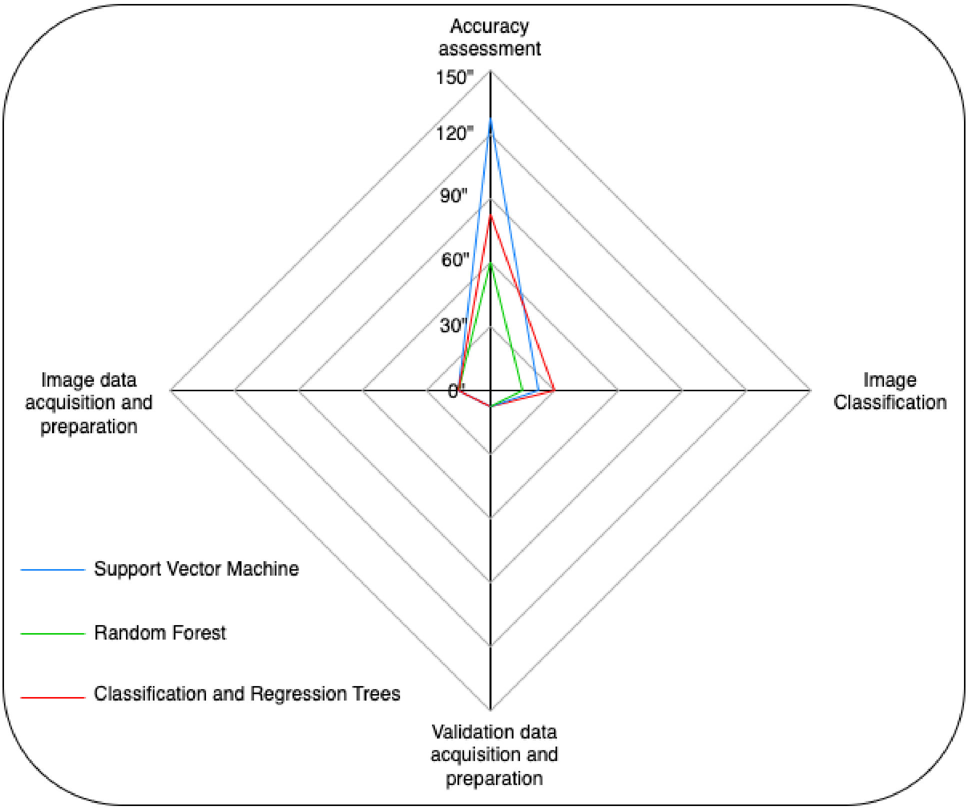

Fig. 6. Distribution of total time in seconds for the four components of mapping model effectiveness (accuracy assessment, image classification, validation data acquisition and preparation, image data acquisition and preparation). Each machine learning model is presented in a different color.

The choice of model for mapping food crops depends on budget, resources, staff expertise, availability of additional imagery and data sets, time constraints (deadlines) and the level of accuracy required [66]. These obstacles are also influenced by the perception of the application of existing food crop maps (paddy) among related parties. Therefore, to produce the most accurate map and in the shortest time, based on this research, it is recommended to apply the RF model. The research findings align with the conclusions of Li et al.., who claimed that RF is appropriate for mapping plants with multiple growing seasons, such rice that is double-cropped [60]. Compared to SVM and CART, the RF model is faster in terms of accuracy assessment and image classification processes (Figure 6). Besides that, the RF model has the highest level of accuracy based on figure 4 and previous research [67], [68].

4 Conclusions

Information regarding the spatial distribution of plants that is current and accurate is vital for both food security and sustainable agricultural management. This study uses machine learning to classify rice crops and shows how effective it is. Try out feature sets using information from satellite photography and three machine learning models, to identify the classification of rice plants in the tropical region of West Java, Indonesia. When it came to feature selection, the NDVI feature produced the best results for plant classification. Among the three machine learning models selected, the RF classifier has the highest achievement, with a 98.51% total accuracy and a high level of effectiveness with the fastest processing in terms of accuracy assessment and image classification. These results show great potential in combining NDVI data with RF algorithms for medium-scale paddy classification research. The techniques used in this study could be modified for use in other plant categorization investigations and greater spatial resolution remote sensing data in the future.

Acknowledgement

Funding this work have been supported by the Center for Higher Education (BPPT) and Indonesia Endowment Funds for Education (LPDP) Number 03412/J5.2.3./BPI.06/10/2022.

References

1. G. Li *et al.*, *Crop type mapping using time-series Sentinel-2 imagery and U-Net in early growth periods in the Hetao irrigation district in China*, Comput Electron Agric, **vol. 203**, p. 107478, (2022), doi: https://doi.org/10.1016/j.compag.2022.107478.
2. M. W. Rosegrant, *Global Food Security: Challenges and Policies*, *Science*, **vol. 302**, no. 5652. pp. 1917–1919, (2003). doi: 10.1126/science.1092958.
3. H. C. J. Godfray, *Food security: The challenge of feeding 9 billion people*, *Science*, **vol. 327**, no. 5967. pp. 812–818, (2010). doi: 10.1126/science.1185383.
4. R. Ridwana, A. Al Kautsar, F. Saleh, S. Himayah, R. Arrasyid, and T. D. Pamungkas, *Spatiotemporal monitoring of rice crops in the covid-19 pandemic period for local food security using sentinel 2b imagery case ctudy: tasikmalaya city*, IOP Conf Ser Earth Environ Sci, **vol. 1089**, no. 1, (2022), doi: 10.1088/1755-1315/1089/1/012039.
5. M. A. M. Javed, A. D. Vishwakarma, S. Ansari, and V. D. Chaudhari, *IoT Based Smart Agriculture System*, International Journal of Innovations in Engineering and Science, **vol. 6**, no. 10, p. 130, (2021), doi: 10.46335/ijies.2021.6.10.27.
6. J. Kent, A. J. Russell, and F. Isaac, *Method and system for agriculture*, US Patent App. 16/960,902, (2020), [Online]. Available: https://patents.google.com/patent/US20200333782A1/en
7. G. Lemaire, *Integrated crop-livestock systems: Strategies to achieve synergy between agricultural production and environmental quality*, Agric Ecosyst Environ, **vol. 190**, pp. 4–8, (2014), doi: 10.1016/j.agee.2013.08.009.
8. U. S. Aliyu, H. Ozdeser, B. Çavuşoğlu, and M. A. M. Usman, *Food security sustainability: A synthesis of the current concepts and empirical approaches for meeting SDGs*, Sustainability (Switzerland), **vol. 13**, no. 21, (2021), doi: 10.3390/su132111728.
9. J. Pretty, *Sustainable intensification in agricultural systems*, Annals of Botany, **vol. 114**, no. 8. pp. 1571–1596, (2014). doi: 10.1093/aob/mcu205.
10. H. Charles, *Food security and sustainable intensification*, Philosophical Transactions of the Royal Society B: Biological Sciences, **vol. 369**, no. 1639, (2014), doi: 10.1098/rstb.2012.0273.
11. U. N. D. of E. and S. Affairs, *The Sustainable Development Goals Report 2019*, United Nations publication issued by the Department of Economic and Social Affairs, p. 64, (2019), [Online]. Available: https://unstats.un.org/sdgs/report/2022/%0Ahttps://www.un-ilibrary.org/content/books/9789210018098%0Ahttps://www.un-ilibrary.org/content/books/9789210478878

12. S. K. Singla, *Spatiotemporal analysis of LANDSAT Data for crop yield prediction*, Journal of Engineering Science and Technology Review, **vol. 11**, no. 3, pp. 9–17, (2018), doi: 10.25103/jestr.113.02.
13. K. Jhajharia, P. Mathur, S. Jain, and S. Nijhawan, *Crop Yield Prediction using Machine Learning and Deep Learning Techniques*, Procedia Comput Sci, **vol. 218**, pp. 406–417, (2023), doi: 10.1016/j.procs.2023.01.023.
14. J. B. Fisher, *The future of evapotranspiration: Global requirements for ecosystem functioning, carbon and climate feedbacks, agricultural management, and water resources*, Water Resources Research, **vol. 53**, no. 4. pp. 2618–2626, (2017). doi: 10.1002/2016WR020175.
15. K. EDJAME, *Potential of Irrigated Crop Water Productivity Mapping to Improving Food and Water Security around Lake Bam, Northwest Burkina Faso*. wascal-togo.org, (2018). [Online]. Available: https://www.wascal togo.org/public/images/publication/Thesis_OUATTARA_MRP_CCHS.pdf
16. O. Rozenstein, N. Haymann, G. Kaplan, and J. Tanny, *Estimating cotton water consumption using a time series of Sentinel-2 imagery, Agric Water Manag*, **vol. 207**, pp. 44–52, Aug. (2018), doi: 10.1016/j.agwat.2018.05.017.
17. K. Li *et al.*, *Dynamic Evaluation of Agricultural Drought Hazard in Northeast China Based on Coupled Multi-Source Data*, Remote Sens (Basel), **vol. 15**, no. 1, (2023), doi: 10.3390/rs15010057.
18. M. Kamal, H. Hartono, P. Wicaksono, N. S. Adi, and S. Arjasakusuma, *Assessment of Mangrove Forest Degradation Through Canopy Fractional Cover in Karimunjawa Island, Central Java, Indonesia*, Geoplanning: Journal of Geomatics and Planning, **vol. 3**, no. 2, p. 107, (2016), doi: 10.14710/geoplanning.3.2.107-116.
19. S. Fraval, *Remote sensing and food security: Monitoring agriculture, ecosystems, hydrology, food environments, and health outcomes*, Proceedings of SPIE - The International Society for Optical Engineering, **vol. 11527**. (2020). doi: 10.1117/12.2576496.
20. P. S. Thenkabail, *Assessing future risks to agricultural productivity, water resources and food security: How can remote sensing help*?, Photogramm Eng Remote Sensing, **vol. 78**, no. 8, pp. 773–782, (2012), [Online]. Available: https://api.elsevier.com/content/abstract/scopus_id/84868009667
21. J. K. Gilbertson and A. van Niekerk, *Value of dimensionality reduction for crop differentiation with multi-temporal imagery and machine learning*, Comput Electron Agric, **vol. 142**, pp. 50–58, (2017), doi: https://doi.org/10.1016/j.compag.2017.08.024.
22. H. Li, C. Zhang, S. Zhang, and P. M. Atkinson, *Full year crop monitoring and separability assessment with fully-polarimetric L-band UAVSAR: A case study in the Sacramento Valley, California*, International Journal of Applied Earth Observation and Geoinformation, **vol. 74**, pp. 45–56, (2019), doi: https://doi.org/10.1016/j.jag.2018.08.024.
23. L. Xun, J. Zhang, D. Cao, S. Zhang, and F. Yao, *Crop Area Identification Based on Time Series EVI2 and Sparse Representation Approach: A Case Study in Shandong Province, China*, IEEE Access, **vol. 7**, pp. 157513–157523, (2019), doi: 10.1109/ACCESS.2019.2949799.
24. L. Zhong, L. Hu, and H. Zhou, *Deep learning based multi-temporal crop classification*, Remote Sens Environ, **vol. 221**, pp. 430–443, (2019), doi: https://doi.org/10.1016/j.rse.2018.11.032.

25. L. Zhong, L. Hu, H. Zhou, and X. Tao, *Deep learning based winter wheat mapping using statistical data as ground references in Kansas and northern Texas, US*, Remote Sens Environ, **vol. 233**, p. 111411, (2019), doi: https://doi.org/10.1016/j.rse.2019.111411.
26. R. Ridwana and S. Himayah, *Utilization of Remote Sensing Technology and Geographic Information Systems for Tourism Development*, International Journal of Applied Sciences in Tourism and Events, **vol. 4**, no. 2, pp. 158–169, (2020), doi: 10.31940/ijaste.v4i2.2042.
27. S. Khanal, K. C. Kushal, J. P. Fulton, S. Shearer, and E. Ozkan, *Remote sensing in agriculture—accomplishments, limitations, and opportunities*, Remote Sens (Basel), **vol. 12**, no. 22, pp. 1–29, (2020), doi: 10.3390/rs12223783.
28. R. P. Sishodia, R. L. Ray, and S. K. Singh, *Applications of remote sensing in precision agriculture: A review (Indices vegetativos utilizados na agricultura)*, Remote Sens (Basel), **vol. 12**, no. 19, pp. 1–31, (2020).
29. M. Wójtowicz, A. Wójtowicz, and J. Piekarczyk, *Application of remote sensing methods in agriculture*, Communications in Biometry and Crop Science, **vol. 11**, no. 1, pp. 31–50, (2016).
30. J. M. Peña-Barragán, M. K. Ngugi, R. E. Plant, and J. Six, *Object-based crop identification using multiple vegetation indices, textural features and crop phenology*, Remote Sens Environ, **vol. 115**, no. 6, pp. 1301–1316, Jun. (2011), doi: 10.1016/j.rse.2011.01.009.
31. I. Kyere, T. Astor, R. Graß, and M. Wachendorf, *Agricultural crop discrimination in a heterogeneous low-mountain range region based on multi-temporal and multi-sensor satellite data*, Comput Electron Agric, **vol. 179**, p. 105864, (2020), doi: https://doi.org/10.1016/j.compag.2020.105864.
32. A. Nemmaoui, M. A. Aguilar, F. J. Aguilar, A. Novelli, and ., *Greenhouse crop identification from multi-temporal multi-sensor satellite imagery using object-based approach: A case study from Almería (Spain)*, Remote Sens (Basel), (2018), [Online]. Available: https://www.mdpi.com/362018
33. M. Kamal, S. Phinn, and K. Johansen, *Assessment of multi-resolution image data for mangrove leaf area index mapping,* Remote Sens Environ, **vol. 176**, pp. 242–254, (2016), doi: 10.1016/j.rse.2016.02.013.
34. R. Ridwana, D. Sugandi, R. Arrasyid, S. Himayah, and T. D. Pamungkas, *Multitemporal landsat image utilization for spatial prediction of built up area in tasikmalaya city, indonesia*, IOP Conf Ser Earth Environ Sci, **vol. 683**, no. 1, (2021), doi: 10.1088/1755-1315/683/1/012101.
35. R. Ridwana *et al.*, *Monitoring Aerosol Optical Depth for Air Quality Through Himawari-8 in Urban Area West Java Province Indonesia*, **vol. 15**, no. 2, (2023), doi: 10.24114/jg.v15i2.36866.
36. Q. HU *et al.*, *How do temporal and spectral features matter in crop classification in Heilongjiang Province, China?*, J Integr Agric, **vol. 16**, no. 2, pp. 324–336, (2017), doi: https://doi.org/10.1016/S2095-3119(15)61321-1.
37. L. H. Samberg, J. S. Gerber, N. Ramankutty, M. Herrero, and P. C. West, *Subnational distribution of average farm size and smallholder contributions to global food production*, Environmental Research Letters, **vol. 11**, no. 12, Nov. (2016), doi: 10.1088/1748-9326/11/12/124010.
38. L. Jia, *Comparative study on crop recognition of LandSat-OLI and RapidEye data*, 6th International Conference on Agro-Geoinformatics, Agro-Geoinformatics 2017. (2017). doi: 10.1109/Agro-Geoinformatics.2017.8047024.

39. F. Arias, M. Zambrano, K. Broce, C. Medina, H. Pacheco, and Y. Nunez, *Hyperspectral imaging for rice cultivation: Applications, methods and challenges*, AIMS Agriculture and Food, **vol. 6**, no. 1, pp. 273–307, (2020), doi: 10.3934/AGRFOOD.2021018.
40. X. Wang, *Crops identification in Kaikong River Basin of Xinjiang based on time series Landsat remote sensing images*, Nongye Gongcheng Xuebao/Transactions of the Chinese Society of Agricultural Engineering, **vol. 35**, no. 16, pp. 180–188, (2019), doi: 10.11975/j.issn.1002-6819.2019.16.020.
41. Z. Yang, Y. Shao, K. Li, Q. Liu, L. Liu, and B. Brisco, *An improved scheme for rice phenology estimation based on time-series multispectral HJ-1A/B and polarimetric RADARSAT-2 data*, Remote Sens Environ, **vol. 195**, pp. 184–201, (2017), doi: https://doi.org/10.1016/j.rse.2017.04.016.
42. X. Huang, J. Wang, J. Shang, C. Liao, and J. Liu, *Application of polarization signature to land cover scattering mechanism analysis and classification using multi-temporal C-band polarimetric RADARSAT-2 imagery*, Remote Sens Environ, **vol. 193**, pp. 11–28, (2017), doi: https://doi.org/10.1016/j.rse.2017.02.014.
43. G. Franceschetti, *Synthetic aperture radar processing*. (2018). doi: 10.1201/9780203737484.
44. D. S. Ladue, P. L. Heinselman, and J. F. Newman, *Strengths and Limitations of Current RADAR Systems for Two Stakeholder Groups in the Southern Plains*, doi: 10.1175/2009BAMS2830.2.
45. A. Veloso, *Understanding the temporal behavior of crops using Sentinel-1 and Sentinel-2-like data for agricultural applications*, Remote Sens Environ, **vol. 199**, pp. 415–426, (2017), doi: 10.1016/j.rse.2017.07.015.
46. O. Csillik, M. Belgiu, G. P. Asner, and M. Kelly, *Object-based time-constrained dynamic time warping classification of crops using Sentinel-2*, Remote Sens (Basel), (2019), [Online]. Available: https://www.mdpi.com/469590
47. Z. Wang, H. Zhang, W. He, and L. Zhang, *Cross-phenological-region crop mapping framework using Sentinel-2 time series Imagery: A new perspective for winter crops in China*, ISPRS Journal of Photogrammetry and Remote Sensing, **vol. 193**, pp. 200–215, (2022), doi: https://doi.org/10.1016/j.isprsjprs.2022.09.010.
48. X. Wu, X. Xiao, Z. Yang, J. Wang, J. Steiner, and R. Bajgain, *Spatial-temporal dynamics of maize and soybean planted area, harvested area, gross primary production, and grain production in the Contiguous United States during 2008-2018*, Agric For Meteorol, **vol. 297**, p. 108240, (2021), doi: https://doi.org/10.1016/j.agrformet.2020.108240.
49. M. G. Maponya, A. van Niekerk, and Z. E. Mashimbye, *Pre-harvest classification of crop types using a Sentinel-2 time-series and machine learning*, Comput Electron Agric, **vol. 169**, Feb. (2020), doi: 10.1016/j.compag.2019.105164.
50. J. Dong, *Mapping paddy rice planting area in northeastern Asia with Landsat 8 images, phenology-based algorithm and Google Earth Engine*, Remote Sens Environ, **vol. 185**, pp. 142–154, (2016), doi: 10.1016/j.rse.2016.02.016.
51. B. D. Wardlow and S. L. Egbert, *Large-area crop mapping using time-series MODIS 250 m NDVI data: An assessment for the U.S. Central Great Plains*, Remote Sens Environ, **vol. 112**, no. 3, pp. 1096–1116, (2008), doi: https://doi.org/10.1016/j.rse.2007.07.019.
52. Y. Chen *et al.*, Mapping croplands, cropping patterns, and crop types using MODIS time-series data, International Journal of Applied Earth Observation and Geoinformation, **vol. 69**, pp. 133–147, (2018), doi: https://doi.org/10.1016/j.jag.2018.03.005.

53. G. Myburgh and A. Van Niekerk, *Effect of Feature Dimensionality on Object-based Land Cover Classification: A Comparison of Three Classifiers*, South African Journal of Geomatics, **vol. 2**, no. 1, pp. 13–27, (2013), [Online]. Available: http://www.sajg.org.za/index.php/sajg/article/view/64
54. P. S. Thenkabail, *Global Cropland-Extent Product at 30-m Resolution (GCEP30) Derived from Landsat Satellite Time-Series Data for the Year 2015 Using Multiple Machine-Learning Algorithms on Google Earth Engine Cloud*, US Geological Survey Professional Paper, **vol. 2021**, no. 1868, pp. 1–63, (2021), doi: 10.3133/pp1868.
55. R. M. A. Latif, J. He, and M. Umer, *Mapping Cropland Extent in Pakistan Using Machine Learning Algorithms on Google Earth Engine Cloud Computing Framework*, ISPRS Int J Geoinf, **vol. 12**, no. 2, (2023), doi: 10.3390/ijgi12020081.
56. J. Yao, J. Wu, C. Xiao, Z. Zhang, and J. Li, *The Classification Method Study of Crops Remote Sensing with Deep Learning, Machine Learning, and Google Earth Engine*, Remote Sens (Basel), **vol. 14**, no. 12, p. 2758, Jun. (2022), doi: 10.3390/rs14122758.
57. A. Htitiou, A. Boudhar, A. Chehbouni, and T. Benabdelouahab, *National-Scale Cropland Mapping Based on Phenological Metrics, Environmental Covariates, and Machine Learning on Google Earth Engine*, Remote Sens (Basel), **vol. 13**, no. 21, p. 4378, Oct. (2021), doi: 10.3390/rs13214378.
58. J. K. Gilbertson, *Effect of pan-sharpening multi-temporal Landsat 8 imagery for crop type differentiation using different classification techniques*, Comput Electron Agric, **vol. 134**, pp. 151–159, (2017), doi: 10.1016/j.compag.2016.12.006.
59. C. Dang, Y. Liu, H. Yue, J. X. Qian, and R. Zhu, *Autumn Crop Yield Prediction using Data-Driven Approaches:- Support Vector Machines, Random Forest, and Deep Neural Network Methods*, Canadian Journal of Remote Sensing, **vol. 47**, no. 2, pp. 162–181, (2021), doi: 10.1080/07038992.2020.1833186.
60. R. Li, *Phenology-based classification of crop species and rotation types using fused MODIS and Landsat data: The comparison of a random-forest-based model and a decision-rule-based model*, Soil Tillage Res, **vol. 206**, (2021), doi: 10.1016/j.still.2020.104838.
61. Y. Liu, D. Xiao, and W. Yang, *An algorithm for early rice area mapping from satellite remote sensing data in southwestern Guangdong in China based on feature optimization and random Forest*, Ecol Inform, **vol. 72**, p. 101853, (2022), doi: https://doi.org/10.1016/j.ecoinf.2022.101853.
62. K. S. Hariyanti, T. June, Y. Koesmaryono, R. Hidayat, and A. Pramudia, *Penentuan Waktu Tanam dan Kebutuhan Air Tanaman Padi, Jagung, Kedelai dan Bawang Merah di Provinsi Jawa Barat dan Nusa Tenggara Timur*, Jurnal Tanah dan Iklim, **vol. 43**, no. 1, pp. 83–92, (2019).
63. X. Wang *et al.*, *Evaluating the Effectiveness of Machine Learning and Deep Learning Models Combined Time-Series Satellite Data for Multiple Crop Types Classification over a Large-Scale Region*, (2022).
64. D. M. W. Powers, *Evaluation: from precision, recall and F-measure to ROC, informedness, markedness and correlation*, pp. 37–63, (2020).
65. D. Lewis, S. Phinn, and L. Arroyo, *Cost-effectiveness of seven approaches to map vegetation communities - A case study from Northern Australia's tropical savannas*, Remote Sens (Basel), **vol. 5**, no. 1, pp. 377–414, (2013), doi: 10.3390/rs5010377.
66. D. Lewis, S. Phinn, and L. Arroyo, *Cost-effectiveness of seven approaches to map vegetation communities - A case study from Northern Australia's tropical savannas*, Remote Sens (Basel), **vol. 5**, no. 1, pp. 377–414, (2013), doi: 10.3390/rs5010377.

67. A. N. L. Winter, *Evaluation and Comparison of Random Forest and Wheat Identification*, (2019).
68. M. Belgiu, *Random forest in remote sensing: A review of applications and future directions*, ISPRS Journal of Photogrammetry and Remote Sensing, **vol. 114**. pp. 24–31, (2016). doi: 10.1016/j.isprsjprs.2016.01.011.